JOURNAL OF GUIDANCE, CONTROL, AND DYNAMICS
Vol. 22, No. 1, January–February 1999

Uncertainty Modeling for Multivariable-Control Robustness Analysis of Elastic High-Speed Vehicles

Frank R. Chavez* and David K. Schmidt†
University of Maryland, College Park, Maryland 20742

High-speed (supersonic or hypersonic) atmospheric flight vehicles are typically characterized by a significant degree of interaction between the highly elastic airframe and the propulsion system. To achieve adequate stability and performance requirements, robust, integrated multivariable control laws will be required. But to apply robust-control analysis or synthesis techniques such as structured-singular-value techniques (μ) or quantitative feedback theory, the uncertainty in the plant dynamics must be characterized in special ways. Furthermore, certain assumptions regarding the uncertainties present are frequently made in the application of these techniques. The focus of this research is the development of uncertainty models for this class of flight vehicle that are derived from the physics of the system, yet are compatible with the cited control synthesis techniques. The potential sources of uncertainty for this class of vehicle are discussed, and three forms of uncertainty models are developed: real parameter, unstructured, and structured. We are especially interested in how the usual sources of uncertainty manifest themselves in this context. It will be shown that for this class of vehicle care is required in making the usual assumptions regarding the uncertainty. It is also shown that the flexible degrees of freedom must be considered in the flight-control synthesis for this class of vehicle.

Nomenclature

A_d	= diffuser area ratio
h	= altitude
I_{yy}	= vehicle y-axis moment of inertia
$K_1(s)$	= control-compensation matrix in feedback path
$K_2(s)$	= control-compensation matrix in the feedforward path
M	= vehicle flight Mach number
$\dot{m}_f$	= fuel mass flow rate
n_x	= axial acceleration
n_z	= normal acceleration
P_2	= combustor inlet pressure
q	= vehicle pitch rate (rigid body)
q_a	= vehicle pitch rate, measured at vehicle aft body location
q_f	= vehicle pitch rate, measured at vehicle forebody location
$\mathrm{Th}_{\mathrm{eng}}$	= engine thrust
u	= vehicle flight velocity
α	= angle of attack (rigid body)
α_m	= angle of attack, measured at vehicle forebody
Δ	= general uncertainty matrix
$\Delta\tau_1$, $\Delta\tau_2$	= elastic mode shape, forebody/afterbody angular deflection
δ_{pitch}	= pitch control surface deflection
ζ	= invacuo elastic mode damping
η	= generalized elastic coordinate
θ	= pitch attitude
ω	= invacuo elastic mode frequency

Introduction

RECENTLY, there has been significant interest in the aerospace community concerning next-generation high-speed atmospheric flight vehicles such as the High-Speed Civil Transport[1] and hypersonic vehicles similar to the National Aerospace Plane (NASP).[2] At issue here is the control of these systems, which have been shown to exhibit a significant degree of dynamic interaction between the elastic airframe and the propulsion system.[3–11] As a result of these interactions it will be necessary to employ multivariable control laws to achieve stability and/or performance requirements imposed on the system.[10,11] An important issue, then, is the robustness of the resulting control law in the presence of vehicle model uncertainty.

In the course of investigating the issues with regard to control laws for these vehicles, researchers have focused a significant effort on characterizing the airframe/engine interactions just noted and on understanding the physical genesis of these interactions.[3,12–16] For example, in a previous paper,[3] the authors have presented an analytical (rather than numerical) model for the flight dynamics of an elastic hypersonic vehicle that includes aeroelastic as well as aeropropulsive interactions characteristic of this class of vehicle. In this paper, the uncertainty characterization, or modeling, for use in multivariable stability/performance robustness analysis is addressed.

The many advances in multivariable robustness theory have been widely reported in the literature and are finding their way into texts and monographs.[17–19] These advances offer the promise of powerful tools for evaluating multivariable systems. But to apply these tools characteristic forms of the model uncertainty are assumed to be available. The existence of a valid uncertainty model in an assumed form is, however, open to question, and this issue has received far less attention in the literature. When uncertainty models are discussed, they are typically overly simplistic and not well supported by the physics of the system under study.

Many research issues remain in the area of uncertainty modeling of real systems, and this paper focuses on several of those issues. For example, the unstructured uncertainty model may not be stable or square, as is typically assumed. Also, the development of a structured uncertainty model may involve several assumptions and approximations that are not true in general. In this investigation, the physical sources of uncertainty for the class of vehicle under study are discussed. Next, three forms of uncertainty models are developed—real parameter, unstructured, and structured—and the necessary assumptions leading to the various models are discussed. These models are then analyzed to further characterize the uncertainty for this vehicular system. It is shown that the parametric uncertainty in the model manifests itself as large uncertainty over a wide frequency range, with peak uncertainty magnitude centered at the modal frequency of the modeled aeroelastic mode. In spite of the fact that the modal frequency and damping are considered uncertain parameters, it is also shown that making a rigid-body assumption for the purpose of control synthesis is not justified for this class

Received Feb. 6, 1997; revision received June 27, 1998; accepted for publication June 27, 1998.

*Doctoral Candidate, Flight Dynamics and Control Laboratory. Student Member AIAA.

†Professor and Director, Flight Dynamics and Control Laboratory. Associate Fellow AIAA.

of vehicle. Finally, a comparison of the relative size of uncertainty arising from the various sources is presented.

Robustness Criteria

For multivariable robustness analysis, the uncertainty must be represented as some form of structured uncertainty, unstructured uncertainty, or some combination.[17–19] As an example in the frequency domain, if G is a system transfer-function matrix, then the following forms of uncertainty are typically considered:

Additive uncertainty:

$$G = \bar{G} + \Delta_a \tag{1a}$$

Input multiplicative uncertainty:

$$G = \bar{G}(I + \Delta_i) \tag{1b}$$

Output multiplicative uncertainty:

$$G = (I + \Delta_o)\bar{G} \tag{1c}$$

where G represents the (uncertain) model of the true system, whereas $\bar{G}$ is the known nominal model for the system. The matrices Δ_a, Δ_i, and Δ_o then represent unstructured or structured uncertainty, where unstructured implies that the elements of Δ_a, Δ_i, and Δ_o are arbitrary, mutually independent, complex numbers, but that the matrix satisfies some bound. For a structured representation of uncertainty, it is assumed that specific sources of uncertainty can be identified and represented, which leads to the matrices Δ_a, Δ_i, and Δ_o taking on a specific structure, such as block diagonal or real valued. For either structured or unstructured uncertainty, Fig. 1 indicates how such uncertainty can be represented in the feedback system, using what is referred to as a linear fractional transformation (LFT).[17,19] Construction of these LFTs will be discussed later.

Stability Robustness

The appropriate multivariable stability criterion depends on the form of uncertainty representation chosen. For example, if the uncertain Δ matrix in Fig. 1 is assumed to be unstructured (i.e., all elements are complex and mutually independent), application of the generalized Nyquist theory leads to the following criteria[17]:

$$\bar{\sigma}(Q_{22}\Delta) < 1, \quad \forall\omega \qquad \text{or} \qquad \bar{\sigma}(Q_{22})\bar{\sigma}(\Delta) < 1, \quad \forall\omega \tag{2a}$$

where $\bar{\sigma}$ denotes the maximum singular value. If the uncertain matrix Δ has some known structure, the Nyquist theory leads to the following stability criteria:

$$\|Q_{22}\|_\mu = \sup_\omega \mu(Q_{22}) < 1/\delta, \qquad \|\Delta\|_\infty \le \delta \tag{2b}$$

where $\mu(Q_{22})$ is the structured singular value of Q_{22} with respect to the structure of Δ, and $\|\Delta\|_\infty = \sup_\omega \bar{\sigma}(\Delta)$.

All of the preceding criteria guarantee, under the usual assumptions of the Nyquist theory, that if the inequality is satisfied, stability of the closed-loop system is assured in the presence of the uncertainty Δ. Note that these inequalities are functions of the uncertainty. Clearly, the larger the uncertainty Δ, the more difficult it will be to satisfy the preceding inequalities for all frequencies. The second of the expressions in Eq. (2a) may be used if nothing is known about the uncertainty other than the bound on Δ. However, this is quite conservative if the actual uncertainty has some structure, which is usually the case.

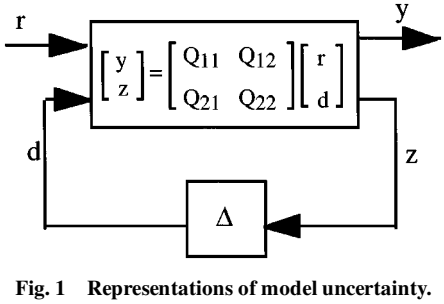

Fig. 1 Representations of model uncertainty.

It is important to recall two necessary assumptions on which the Nyquist theory depends: that the nominal closed-loop system is stable and that over the range of the uncertainty the number of unstable poles of the system remains invariant.[17] Frequently, this latter assumption is guaranteed under the more restrictive assumption that the uncertainty Δ is stable. Finally, a third assumption regarding the structured uncertainty model, independent from the preceding ones, is that the sources of uncertainty are independent. (Note here the various assumptions regarding existence and properties of the uncertainty.)

Performance Robustness

Criteria for performance robustness (which includes stability robustness as a requirement) may also be cast in a form consistent with the preceding criteria.[17,18] The feedback system including the uncertainty may again be considered in the form shown in Fig. 1. Note the inputs and outputs $\boldsymbol{r}$ and $\boldsymbol{y}$ are not necessarily the same as those used for the stability robustness analysis, and so the matrix Q may be different. Here the inputs and outputs are chosen such that the performance specification may be stated in the following form:

$$\|Q_{11}\|_\infty < 1$$

As discussed in Ref. 17 or 19, by adding a fictitious uncertainty block Δ_o between the output $\boldsymbol{y}$ and the input $\boldsymbol{r}$, a performance robustness criterion may be stated in the form

$$\|Q\|_\mu < 1$$

with respect to the structure of $\tilde{\Delta} = \text{diag}\{\Delta_o, \Delta\}$. But again the uncertainty must be characterized such that the system may be represented as in Fig. 1.

Therefore, if the uncertainty can be characterized in a form consistent with the preceding criteria, these stability/performance criteria can be used to evaluate the stability/performance robustness of the multivariable control system.

Constructing the Linear Fractional Transformation and Scaling

The stability criteria of Eqs. (2a) and (2b) assume the feedback system may be represented as an LFT. In this section, obtaining the LFT will be discussed. Assume the nominal system model to be used in the control law synthesis is denoted $\bar{G}$, with state-space realization $[\bar{A}, \bar{B}, \bar{C}, \bar{D}]$. Furthermore, assume the control law to have the fairly general form $\boldsymbol{u} = -K_1(s)\boldsymbol{y} + K_2(s)\boldsymbol{e}$. Finally, $\boldsymbol{e}$ is the output error, or $\boldsymbol{e} = \boldsymbol{r} - \boldsymbol{y}$.

Stability Robustness Against Unstructured Uncertainty

To apply the criteria in Eq. (2a) the appropriate Q_{22} matrix must be developed. The closed-loop system and an additive unstructured uncertain matrix Δ_a is shown in Fig. 2. After some block diagram algebra, the following Q_{22} transfer function matrix is obtained:

$$Q_{22} = -[I + (K_1 + K_2)\bar{G}]^{-1}(K_1 + K_2)$$

Now consider the criteria for guaranteed stability consisting of the first of Eq. (2a) with Δ taken to be Δ_a. The maximum singular value on the left of the inequality depends on the units of the input and output signals of the system G. One approach to minimize conservatism in this stability criterion is to insert scaling matrices, as shown by the dashed blocks of Fig. 2, and to select the scaling to minimize the maximum singular value at each frequency. (Usually this selection is based on minimization of the Frobenius norm of the matrix in question, which is computationally more straightforward.) Again, if Δ_a were a square matrix, then selecting $D_{\text{in}} = D_{\text{out}} = D$ leads to a single robustness criterion involving D. However, in many practical situations, Δ_a is not square, in which case $D_{\text{in}} \neq D_{\text{out}}$.

The stability robustness criterion of Eq. (2a), in conjunction with Fig. 2, results from breaking the feedback loop at the input to Δ_a and the matrix $(Q_{22}\Delta_a)$ is a square matrix. Similarly, breaking the

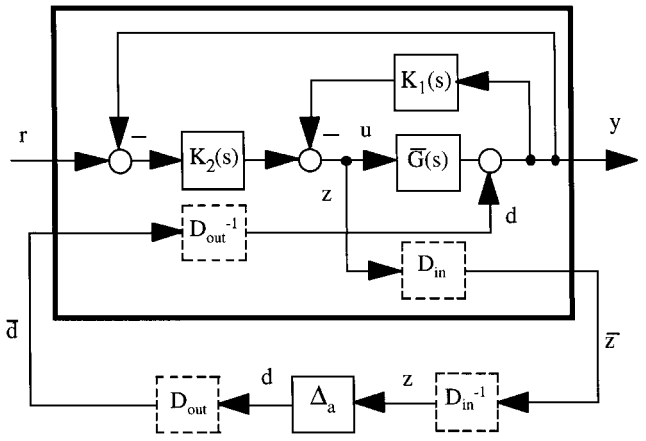

Fig. 2 System representation with unstructured uncertainty.

feedback loop at the output of Δ_a will yield another stability robustness criterion involving another square matrix, namely, $(\Delta_a Q_{22})$. By using the two scaling matrices D_{in} and D_{out}, one obtains two stability robustness criteria in which the appropriate scaling matrix is used. Breaking the loop at $\bar{z}$ results in the following input stability criteria:

$$\inf_{D_{\text{in}}} \left\{ \sup_{\Delta_a \in \Delta_a^*} \bar{\sigma}\left(D_{\text{in}} Q_{22} \Delta_a D_{\text{in}}^{-1}\right) \right\} < 1, \quad \forall \omega \tag{3a}$$

$$D_{\text{in}} \in \{\text{diag}[1, d_1, d_2];\ d_i \in \mathbb{R},\ i = 1, 2\}$$

whereas breaking the loop at $\bar{d}$ results in the following output stability criteria:

$$\inf_{D_{\text{out}}} \left\{ \sup_{\Delta_a \in \Delta_a^*} \bar{\sigma}\left(D_{\text{out}} \Delta_a Q_{22} D_{\text{out}}^{-1}\right) \right\} < 1, \quad \forall \omega \tag{3b}$$

$$D_{\text{out}} \in \{\text{diag}[1, d_1, d_2, d_3, d_4, d_5, d_6, d_7];\ d_i \in \mathbb{R},\ i = 1, 2, \ldots, 7\}$$

In Eqs. (3a) and (3b), the Δ_a is selected to maximize the singular value, whereas the D scalings are selected to minimize the singular value for the selected Δ_a. Finally, because the criteria in Eqs. (3a) and (3b) are sufficient conditions for stability robustness, stability is guaranteed if either of these two criteria is satisfied.

Stability Robustness Against Structured Uncertainty

For the structured uncertainty model to be presented, the system open-loop transfer-function matrix can be represented as

$$\begin{bmatrix} y \\ z \end{bmatrix} = \begin{bmatrix} P_{11} & P_{12} \\ P_{21} & P_{22} \end{bmatrix} \begin{bmatrix} u \\ d \end{bmatrix}$$

where

$$P_{11} = \bar{G}, \qquad P_{12} = \bar{C}(sI - \bar{A})^{-1} U_1 + U_2$$

$$P_{21} = V_1^T (sI - \bar{A})^{-1} \bar{B} + V_2^T, \qquad P_{22} = V_1^T (sI - \bar{A})^{-1} U_1$$

and the matrices U_1, U_2, V_1, and V_2 will be defined in Eq. (7) in a later section. The Q_{22} matrix now becomes

$$Q_{22} = P_{22} - P_{21}[I + (K_1 + K_2)P_{11}]^{-1}(K_1 + K_2)P_{12}$$

Under the condition that $\|\Delta\|_\infty < \delta$, Eq. (2b) guarantees stability in the presence of the uncertainty Δ (Ref. 17), where $\mu(Q_{22})$ is the structured singular value of Q_{22} with respect to the structure of Δ to be presented in Eq. (8).

One approximation for $\mu(Q_{22})$, similar to the D scaling used earlier, is

$$\mu(Q_{22}) \le \inf_D \bar{\sigma}\left(D Q_{22} D^{-1}\right)$$

where D here has the same block diagonal structure as Δ. Another easily computed approximation can also be used here because the blocks that make up Δ are scalar.[17,20] This approximation is

$$\mu(Q_{22}) \le \inf_D \bar{\sigma}\left(D Q_{22} D^{-1}\right) \le \bar{\lambda}(|Q_{22}|)$$

where $\bar{\lambda}(|Q_{22}|)$ is the maximum eigenvalue of the absolute value (or the Perron eigenvalue) of Q_{22}.

Study Vehicle and Sources of Uncertainty

A generic hypersonic vehicle with geometry similar to that of the X-30[2] is to be considered as an example case study. The numerical results to be presented correspond to a vehicle configuration similar to that considered in Ref. 3, where in this model only one elastic degree of freedom is included. The vehicle's geometry and mass properties are as follows: vehicle length = 150 ft, $\omega = 18$ rad/s, weight = 300,000 lb, $\zeta = 0.02$, $I_{yy} = 20 \times 10^6$ slug-ft^2, and $\Delta\tau_1 = \Delta\tau_2 = 1$ deg. The linearized dynamics, referenced to a Mach 8 steady level flight condition at 100,000-ft altitude, are given in Appendix A.

The forces and moments on the vehicle arise due to the pressure distribution acting over the surface, which is due to aerodynamic and propulsive effects. These forces and moments are then functions of dynamic pressure, Mach number, vehicle geometry, structural deformation, and orientation of the vehicle with respect to the relative wind vector. As shown in Ref. 3, the resulting dynamics are expressible, after linearization, in terms of over 25 different stability derivatives. In Ref. 3, analytical expressions were derived for all of the stability derivatives. These expressions are nonlinear functions of vehicle geometry and mass properties, atmospheric pressure, structural-vibration mode shapes, and flight Mach number.

The system dynamics are also a function of the invacuo structural-vibration modal frequencies ω and dampings ζ. For example, two elements of the system dynamic matrix in Appendix A are given next as

$$A(7, 6) = (1/m^*)\mathcal{F}_\eta - \omega^2, \qquad A(7, 7) = (1/m^*)\mathcal{F}_{\dot{\eta}} - 2\xi\omega \tag{4}$$

It is further noted that the system-dynamic matrices A and B are full, and therefore the elastic and rigid-body degrees of freedom are fully coupled. This is in contrast to models of isolated elastic structures that are frequently expressed as diagonal systems exhibiting little coupling. Finally, the mode shapes appear throughout the system's A, B, C, and D matrices because the surface pressures arising from aerodynamic and propulsive effects are dependent on the vehicle shape, which is in turn affected by the vehicle's elastic deformation.

Therefore, one important source of uncertainty is the vehicle's structural dynamic characteristics. First, any neglected elastic degrees of freedom would constitute unmodeled dynamics, and to assume that the vehicle is rigid would be to neglect all elastic degrees of freedom. Furthermore, any elastic degrees of freedom that are included in the model are imperfectly modeled, giving rise to errors (or variations from nominal) in the invacuo structural mode shapes, vibration modal frequencies ω, and dampings ζ. Variations in these parameters are of course due to variations in the mass and stiffness properties of the structure and/or errors in the model of these structural properties. Note here that these parameters are not strictly mutually independent because they all depend on the structural-stiffness and mass distributions. However, if the mass and stiffness matrices may vary due to a variety of reasons (e.g., changes in mass distribution or vehicle configuration), the modal parameters may reasonably be assumed to be independent if the variations are sufficiently small.

Other sources of uncertainty are the errors in predicting (or variations from nominal in) the pressure distribution that, when integrated, leads to the generalized forces and moments acting on the elastic structure. Such errors lead directly to errors in the stability derivatives, as expressed in Eqs. (4), for example. One could attempt to model this uncertainty as variations in the vehicle's stability derivatives, as in Ref. 21. However, the stability derivatives are not mutually independent either because all depend on the pressure

distribution. However, some stability derivatives may be assumed independent, such as those modeling the control power (force or moment) of an aerodynamic control surface.

The pressure distribution, considered as the source of uncertainty, is expressible in terms of the freestream pressure P_∞ modified by a spatially varying pressure coefficient $C_p(x, y, z)$. One could then, for example, treat variations in pressure distribution as a (real or fictitious) variation in P_∞ or as functional variations in the pressure coefficient, depending on the true source of uncertainty being modeled.

Until now, we have discussed sources of uncertainty associated with the aerodynamic and structural dynamic characteristics of the system. There is, of course, uncertainty associated with modeling of the propulsion subsystem. As shown in Ref. 3, the combustor inlet pressure and engine thrust are functions of the engine inlet conditions and the engine control inputs: diffuser area ratio and fuel mass flow rate. The inlet conditions to the engine depend on the aerodynamics and structural dynamics of the vehicle forebody; hence, uncertainty in the inlet conditions has already been accounted for. Additional uncertainty associated with the propulsion system may be represented as uncertainty in engine control power.

A fourth source of uncertainty is the variation in mass properties over the flight envelope, including the generalized masses of any modeled elastic degrees of freedom. These mass properties appear as lumped parameters in the model and affect all of the stability derivatives.

Although not exhaustive, this discussion highlights the major sources of uncertainty in the vehicle airframe model. Uncertainties in the sensors, actuators, and control hardware have not been addressed but may also be significant.

Uncertainty Model

Parameter Uncertainty

Based on the preceding discussion, the following parameters could be considered as uncertain: freestream atmospheric pressure P_∞; surface pressure coefficient $C_p(x, y, z)$; aerodynamic and propulsive control power coefficients $()_{\delta_{\text{pitch}}}$, $()_{\text{Ad}}$, and $()_{\dot{m}_f}$, respectively; structural mode frequency, damping, and mode shape ω, ζ, $\Delta\tau_1$, and $\Delta\tau_2$, respectively; and mass, inertias, and generalized masses m, I_{yy}, and m^*, respectively.

Let the parameter uncertainty, in general, be denoted as a vector of uncertain parameters $\boldsymbol{p}$. In the numerical results to follow, the following parameters are treated as uncertain and are assumed to lie within the following ranges (here an uncertainty of 10 or 20% is assumed, based on limited experience with this class of vehicle; as more experimental and analytical data become available for these systems, better estimates of the anticipated uncertainty should be developed): $\boldsymbol{p}_1 = \{P_\infty, \omega, \zeta, \Delta\tau_1, \Delta\tau_2\}$ — ±10% of nominal value, and $\boldsymbol{p}_2 =$ {elevator control power, diffuser control power, fuel flow control power} — ±20% of nominal.

Unstructured Form of Uncertainty

If the system transfer-function matrix G is square and invertible, any of the forms of unstructured uncertainty model discussed in earlier sections may be used. Frequently, applications of multivariable robustness theory treat only square systems. However, in many cases, two or more measured outputs may be blended to form a single feedback signal to a particular control input, which gives rise to a nonsquare system matrix. For example, in Ref. 6 forebody pitch rate, aft body pitch rate, and normal acceleration measurements are blended and fed back to the pitch control input for attitude stabilization and structural mode augmentation. It might be argued that this blended output can be incorporated into the system transfer function matrix to form an equivalent square system. But in general this is not appropriate because constants or compensators used in the blending are control law dependent. Therefore, if G for the system under consideration is not square, only the additive form of uncertainty Δ_a, Eq. (1), may be used.

The additive uncertainty matrices Δ_a to be obtained will include effects of both neglected dynamics as well as parameter uncertainty. The technique is as follows. Variations in the parameter vector of interest $\boldsymbol{p}$ give rise to variations in the system's state-space quadruple, $[A, B, C, D]$, or equivalently in the system transfer-function matrix, $G = C(sI - A)^{-1}B + D$. Let the nominal values for the parameters be denoted $\bar{\boldsymbol{p}}$, which in turn leads to the nominal system model $\bar{G}$. Then if the actual system is denoted as G, which reflects the true (but unknown) set of parameter values $\boldsymbol{p}$ plus all unmodeled dynamics, an additive uncertainty matrix Δ_a is defined from the relation $\Delta_a = G - \bar{G}$. However, a numerical realization for such a Δ_a may not actually be obtained, and so the following approximation will be used. The parameters in $\boldsymbol{p}$ are treated here as uncertain but are known to lie in a given range. Let a given set of values for the parameters in $\boldsymbol{p}$ be denoted as $\boldsymbol{p}^i$, and the associated model be denoted as G^i. Then as the parameters in $\boldsymbol{p}$ are varied over their respective range, a set of Δ_a (each found from a G^i) will be generated. Let this set be denoted as Δ_a^*. This uncertain set is taken to be the additive form of the uncertainty model. It is an uncertain matrix for which a bound may be estimated. Finally, a finite set of unmodeled degrees of freedom may be specifically treated in this fashion by including them in each G^i generated as before.

If the bound is taken as the maximum singular value of a matrix $\bar{\sigma}()$, then for each $\boldsymbol{p}^i$ (and associated G^i) the $\bar{\sigma}(\Delta_a)$ may be found. If this process is repeated over the range of parameters $\boldsymbol{p}$, and over a range of frequencies, then the bound

$$\bar{\sigma}\left(\Delta_a^*\right) \equiv \sup_{\boldsymbol{p}^i} \bar{\sigma}(\Delta_a) \tag{5}$$

may be estimated numerically and plotted as a function of frequency.

Although variations in $\boldsymbol{p}$ may be the genesis of an uncertain matrix Δ_a^*, this matrix will have no specific structure. It will be fully populated with complex elements. However, the elements are not all truly mutually independent, and so here we will consider a Δ_a^* generated in this fashion as a special unstructured representation of the parameter uncertainty. Such an additive unstructured uncertainty model may be used to represent unmodeled dynamics, as well as errors, or variations, in system parameters. One application of this additive unstructured uncertainty model is in the determination of the frequency range where the uncertainty may be largest.

Structured Form of Uncertainty

If the uncertain parameters appear linearly in the system model or if a block diagram or signal flow graph can be constructed for the system, and if the uncertain parameters are mutually independent, then an uncertainty matrix Δ can be constructed that will have a block diagonal structure.[17,19,20] Rather than use the block diagram approach, as in Ref. 20, for example, an alternate technique will be developed.

From Ref. 3 and the discussion in the previous section we note that, except for the modal damping, atmospheric pressure, and control-power coefficients, the uncertain parameters considered here appear neither linearly nor in a consistent form (i.e., in the same algebraic or trigonometric form) in the system-dynamic model. As a result, uncertainties in the parameters in these expressions cannot be expressed as simply additive uncertainty in some matrix (i.e., $A = \bar{A} + \delta\Delta_a$) or as multiplicative uncertainty in some matrix (i.e., $A = \bar{A}[I + \delta\Delta_m]$), where $\bar{A}$ is the nominal system dynamic matrix and δ represents some parametric uncertainty.

However, an approximate structured uncertainty representation can be obtained. Let the parameter vector $\boldsymbol{p}$ include the uncertain parameters in the system. As a specific example, let $\boldsymbol{p} = \boldsymbol{p}_1 = \{P_\infty, \omega, \zeta, \Delta\tau_1, \Delta\tau_2\}$, and let variations in these parameters be expressed as $\delta\boldsymbol{p} = \{\delta p_1, \delta p_2, \delta p_3, \delta p_4, \delta p_5\}$ where

$$\delta p_1 = \frac{P_\infty - \bar{P}_\infty}{\bar{P}_\infty}, \qquad \delta p_2 = \frac{\omega - \bar{\omega}}{\bar{\omega}}, \qquad \delta p_3 = \frac{\zeta - \bar{\zeta}}{\bar{\zeta}}$$

$$\delta p_4 = \frac{\Delta\tau_1 - \overline{\Delta\tau_1}}{\overline{\Delta\tau_1}}, \qquad \delta p_5 = \frac{\Delta\tau_2 - \overline{\Delta\tau_2}}{\overline{\Delta\tau_2}}$$

Now the system matrices $[A, B, C, D]$ may be expanded in a Taylor series in terms of these parameter variations. Assuming further that the real parameter variation is small, or $\delta p_i \ll 1$, for all i, we may

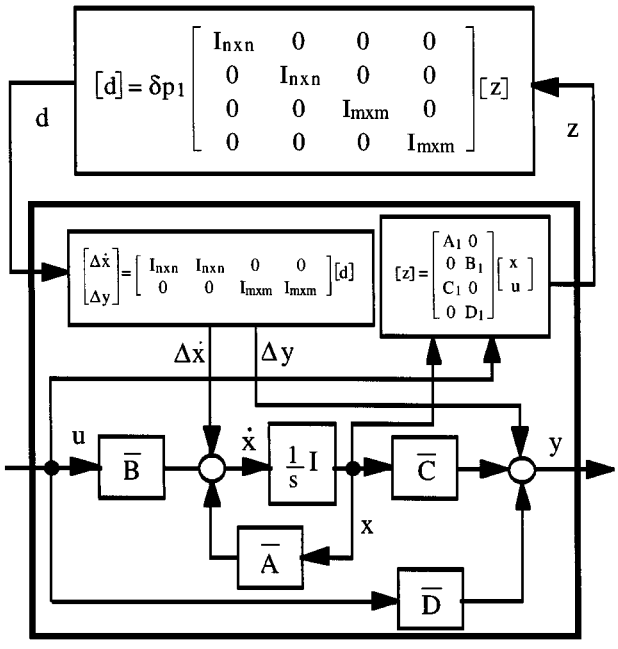

Fig. 3 Single-parameter structured uncertainty.

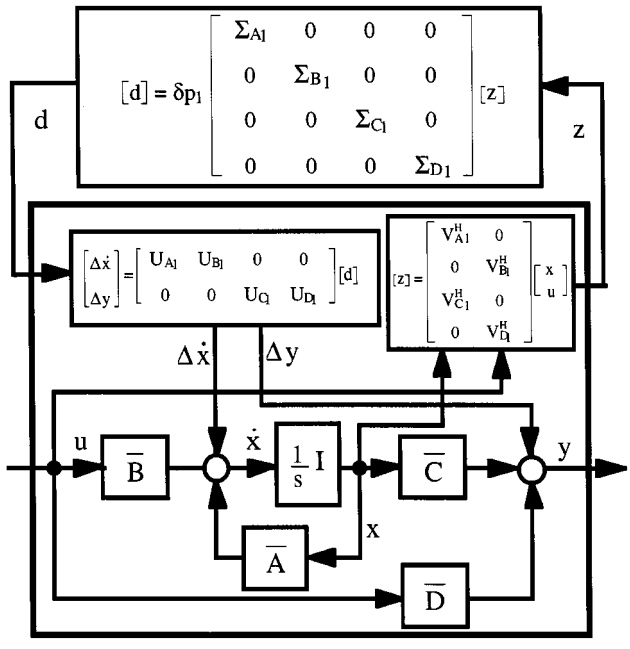

Fig. 4 Real parameter structured uncertainty—singular value decomposition.

retain only the first-order terms in the series as significant. This yields the following:

$$A = \bar{A} + \sum_{i=1}^{5} \delta p_i A_i, \qquad B = \bar{B} + \sum_{i=1}^{5} \delta p_i B_i$$

$$C = \bar{C} + \sum_{i=1}^{5} \delta p_i C_i, \qquad D = \bar{D} + \sum_{i=1}^{5} \delta p_i D_i \tag{6}$$

where the overbar indicates the nominal system matrices, and, for example,

$$A_i = \frac{\partial A}{\partial \delta p_i}$$

Now, assume for the moment that there is only one uncertain parameter δp_1. This uncertainty can be isolated as in Fig. 3. Comparing this figure with Fig. 1, one sees that this real parameter uncertainty may be represented as

$$\Delta = \delta p_1 I_{(2n+2m)\times(2n+2m)}$$

where n is the number of states and m is the number of outputs. For the vehicle model being considered, $n = 7$ and $m = 8$. Hence, the size of this uncertainty block is 30×30.

Suppose further that the only element in the system that depends on p_1 is the i, jth element of A, or $A(i, j)$. In this case, the elements of the matrix A_1 in Eq. (6) are all zero except for element i, j. Therefore, the uncertainty in the A matrix due to the uncertainty in the real parameter δp_1 can be represented as

$$\delta p_1 A_1 = \hat{e}_i [\delta p_1 A_1(i, j)] \hat{e}_j^T$$

where $\hat{e}_i$ is the ith basis vector.

This suggests that it is not necessary to use a full 7×7 identity matrix to represent $\delta p_1 A_1$ as indicated in Fig. 3. One method for minimizing the number of repeated entries in the structured uncertainty block Δ is to express the matrices A_1, B_1, C_1, and D_1 in terms of their singular value decomposition (e.g., $A_1 = U_{A_1} \Sigma_{A_1} V_{A_1}^H$), as shown in Fig. 4 (Ref. 20). Here, Σ_{A_1} contains only the nonzero singular values of A_1. The uncertainty can now be expressed as

$$\Delta = \delta p_1 I_{r_1 \times r_1}$$

$$r_1 = \text{rank}(A_1) + \text{rank}(B_1) + \text{rank}(C_1) + \text{rank}(D_1) \le 2n + 2m$$

and the number of repeated entries in the structured uncertainty block Δ is minimized.

Consider now all of the uncertain parameters $\boldsymbol{p}$. The system, including the uncertainty, can be expressed as

$$\dot{\boldsymbol{x}} = \bar{A}\boldsymbol{x} + \bar{B}\boldsymbol{u} + U_1\boldsymbol{d}, \qquad \boldsymbol{y} = \bar{C}\boldsymbol{x} + \bar{D}\boldsymbol{u} + U_2\boldsymbol{d}$$

$$\boldsymbol{z} = V_1^T\boldsymbol{x} + V_2^T\boldsymbol{u}$$

where the matrices U_1, U_2, V_1, and V_2 are given by

$$U_1 = \begin{bmatrix} U_{A_1} & U_{B_1} & 0 & 0 & \cdots & U_{A_5} & U_{B_5} & 0 & 0 \end{bmatrix}$$

$$U_2 = \begin{bmatrix} 0 & 0 & U_{C_1} & U_{D_1} & \cdots & 0 & 0 & U_{C_5} & U_{D_5} \end{bmatrix}$$

$$V_1 = \begin{bmatrix} V_{A_1}\Sigma_{A_1} & 0 & V_{C_1}\Sigma_{C_1} & 0 & \cdots & V_{A_5}\Sigma_{A_5} & 0 & V_{C_5}\Sigma_{C_5} & 0 \end{bmatrix}$$

$$V_2 = \begin{bmatrix} 0 & V_{B_1}\Sigma_{B_1} & 0 & V_{D_1}\Sigma_{D_1} & \cdots & 0 & V_{B_5}\Sigma_{B_5} & 0 & V_{D_5}\Sigma_{D_5} \end{bmatrix} \tag{7}$$

For the vehicle model considered herein, and if $\boldsymbol{p}$ is taken to be $\boldsymbol{p}_1$, numerical values for the preceding matrices are given in Appendix B. Further, the structured uncertainty block Δ (see Fig. 1) relating the disturbance input vector $\boldsymbol{d}$ to the output vector $\boldsymbol{z}$ has the following block diagonal form:

$$\Delta = \text{diag}\{\delta_{p_1} I_{11\times 11}, \delta p_2, \delta p_3, \delta p_4 I_{5\times 5}, \delta p_5 I_{5\times 5}\} \tag{8}$$

Note that the structural-mode frequency and damping parameter uncertainty, δp_2 and δp_3, respectively, appear with a multiplicity of 1, whereas the atmospheric-pressure uncertainty, δp_1, and mode-shape parameter uncertainties, δp_4, and δp_5, enter as repeated blocks. Recall that δp_1, δp_4, and δp_5 are lumped-parameter representations of uncertain aerodynamic/propulsive pressure and mode-shape distributions.

The structured-uncertainty form more precisely captures uncertainty arising due to variations in lumped parameters. It is important to note that in the development of this model form we were significantly aided by the availability of an analytic vehicle model from Ref. 3. Furthermore, as mentioned earlier, the uncertainties are limited to small perturbations in the parameters.

Analysis of the Uncertainty Models

Even though the robustness criteria, Eqs. (2), are for the closed-loop system, analysis of the unstructured uncertainty models of the open-loop system can be informative. In the first such analysis, let $\boldsymbol{p} = \{p_1, p_2\}$, and consider 200 randomly generated sets of values of these parameters (i.e., $\boldsymbol{p}^i$: $i = 1, \ldots, 200$), each parameter lying in its respective allowable range.

The bound on the uncertain matrix Δ_a^*, determined from Eq. (5), is plotted in Fig. 5 for $\boldsymbol{p} = \{\boldsymbol{p}_1, \boldsymbol{p}_2\}$. Also shown in this figure is the same bound if only one source of uncertainty is considered. This comparison gives information regarding the contribution of each of the sources of uncertainty to the total aggregate uncertainty. This total uncertainty is quite large compared with the magnitude of $\bar{\sigma}[\bar{G}(j\omega)]$, especially near the aeroelastic-mode frequency of 18 rad/s. Of course, larger uncertainty implies greater difficulty in satisfying the criteria in Eqs. (2).

One frequently made assumption in the application of the stability criteria in Eqs. (2) is that of a stable Δ_a. This of course assumes that the uncertainty does not change the number of unstable poles of the plant. However, due to the manner in which Δ_a^* was derived here, it should be clear that this Δ_a will not be stable. In fact, each Δ_a in Δ_a^* has eigenvalues that include those of the nominal unstable plant. Hence the frequently made assumption of a stable Δ_a is violated. However, to apply the Nyquist theory, one only requires invariance of the number of unstable poles in G, over the range of parameter uncertainty considered. Based on numerical results obtained here, this requirement appears to be satisfied, though all of the members in the set Δ_a^* are not stable. This tentative conclusion is based on an eigenanalysis of all G^i; $i = 1, \ldots, 200$. Of course, to perform such an analysis requires all G^i to be available, which is a limitation. Consequently, for performance of Nyquist-based stability analysis on this class of vehicle with parameter uncertainty, use of the structured-uncertainty form would appear more appropriate.

As a second case analysis we will consider unmodeled dynamics or, more specifically, neglected structural dynamics. The question is whether one should use a model that includes structural dynamics when these dynamics are uncertain or just to use a rigid-body assumption and not to include elastic degrees of freedom in the nominal model.

Now, consider the same true system G used in the previous analysis. Again, this system includes the modeled flexible degrees of freedom with the uncertain parameters $\boldsymbol{p} = \boldsymbol{p}_1$. Also, we now take the nominal or design system model to be G_{rigid}, the plant transfer-function matrix obtained by eliminating the structural-dynamic degrees of freedom via residualization. Finally, define, as before, $\bar{G}$ to be the transfer-function matrix of the vehicle including the modeled flexible degrees of freedom.

Therefore the additive uncertainty arising only due to neglecting the structural dynamics (ignoring parameter uncertainty for now) is

$$\Delta_{\text{rigid}} = \bar{G} - G_{\text{rigid}}$$

and the difference between the true system and the rigid-body model, $G - G_{\text{rigid}}$, may be expressed as

$$G - G_{\text{rigid}} = (G - \bar{G}) + (\bar{G} - G_{\text{rigid}})$$

By observation, one sees that the uncertainty matrix associated with using a rigid-body model in this situation, denoted as $\Delta_{a+\text{rigid}}^*$, is then

$$\Delta_{a+\text{rigid}}^* = \Delta_a^* + \Delta_{\text{rigid}}$$

where Δ_a^* and Δ_{rigid} are as defined previously.

A plot of the bound of this uncertain matrix is shown in Fig. 6, in which this bound is again compared with that for parameter uncertainty only, or Δ_a^*. Here the error introduced by the rigid-body assumption is clearly identified. This error significantly increases the uncertainty above $\omega = 1$ rad/s, although at the nominal frequency of the aeroelastic mode (18 rad/s) both uncertainty models are about 40 dB in magnitude. The greater uncertainty above 1 rad/s is important because the unstable mode for this study vehicle is at about 1.3 rad/s, and to stabilize this mode will require gain crossover to be at least this frequency. Based on these results, it would appear

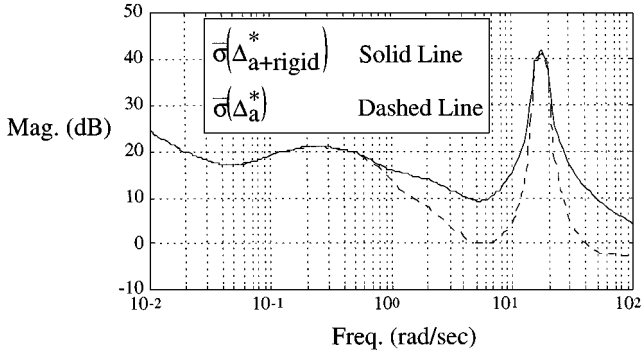

Fig. 6 Parametric and parametric + rigid unstructured uncertainty bounds.

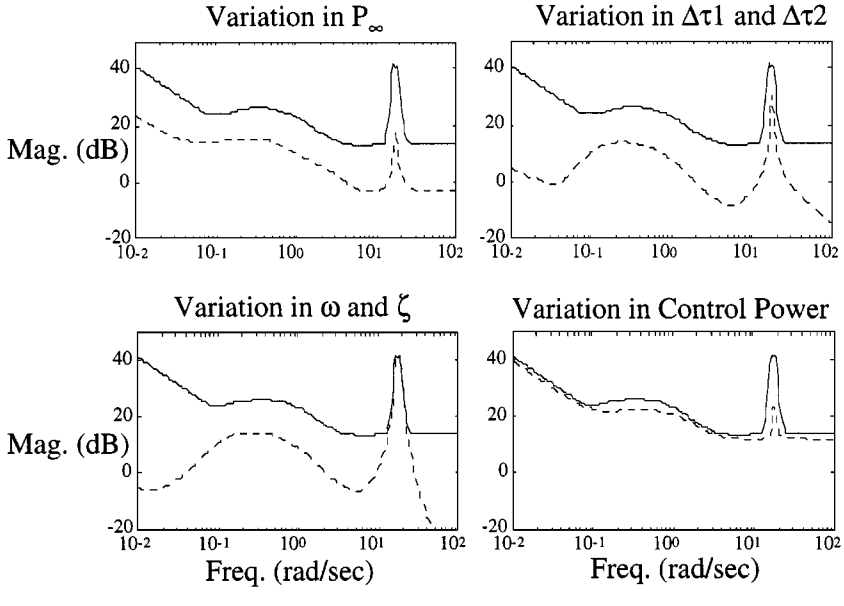

Fig. 5 Bound on the additive uncertainty: ——, total uncertainty; – – –, individual uncertainty source.

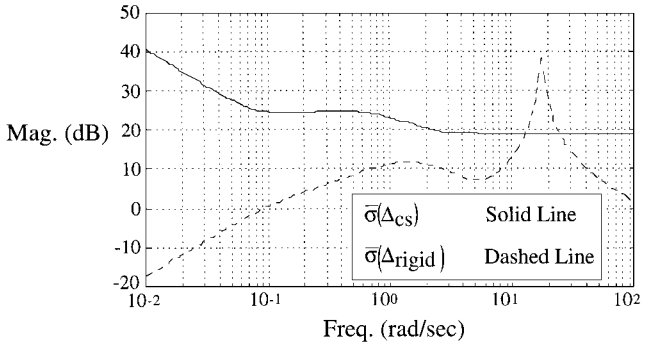

Fig. 7 Control effectiveness and rigid unstructured uncertainty bounds.

that the use of a flexible model is important here even if that model has uncertain modal characteristics.

As a third case analysis, consider the uncertainty introduced due to uncertain control-power coefficients, or $\boldsymbol{p} = \boldsymbol{p}_2 =$ {elevator control power, diffuser control power, fuel-flow control power}. If the true system is assumed to be rigid and only $\boldsymbol{p}_2$ is uncertain, similar to the case in Ref. 7, for example, the additive uncertainty matrix would be

$$\Delta_{cs} = G_{\text{rigid}} \begin{bmatrix} \pm 0.2 & & \\ & \pm 0.2 & \\ & & \pm 0.2 \end{bmatrix}$$

This additive uncertainty reflects the 20% parameter uncertainty in $\boldsymbol{p}_2$.

Now, two modeling approaches will be compared in terms of the amount of uncertainty introduced. One modeling approach assumes a rigid vehicle with uncertain $\boldsymbol{p}_2$, which leads to the preceding uncertainty model Δ_{cs}. The second approach assumes known $\boldsymbol{p}_2$ but includes the uncertainty due to the rigid-body assumption, which leads to the uncertainty Δ_{rigid} defined earlier. The maximum singular values of Δ_{rigid} and Δ_{cs} are shown in Fig. 7. It is clear that in the frequency range of the vehicle's aeroelastic mode the uncertainty associated with control effectiveness is smaller than the uncertainty associated with neglecting the structural dynamics, whereas at other frequencies the control-power uncertainty is larger. Hence, a control law synthesized under a rigid-body assumption may not be robust against these unmodeled elastic effects, even though it may be robust against control-power uncertainty.

Conclusion

The focus of this research is the development of uncertainty models, particularly for a class of flexible, high-speed atmospheric flight vehicles. These uncertainty models are required before modern, multivariable robust control techniques may be applied. The potential sources of uncertainty for these vehicular systems is identified as uncertain aerodynamic and structural-dynamic modeling. Three different forms of uncertainty models were developed: a real parameter, an unstructured, and a structured uncertainty model. However, to derive these models from the physics, it was noted that several assumptions were necessary. The uncertain parameters were assumed to be independent, the uncertainty was small compared with the nominal values of the parameters, and that uncertain aerodynamic and structural-dynamic modeling can in fact be appropriately represented as uncertainty in a lumped parameter. Also, some frequently made assumptions concerning properties of the uncertainty model were found to be violated. For example, the unstructured uncertainty model developed for this class of vehicle is unstable. Hence, assumptions made about the existence and properties of such uncertainty models for some arbitrary flight system may not be justified.

It was shown that the parametric uncertainty considered herein manifests itself as large uncertainty over a wide frequency range, with peak uncertainty magnitude centered at the modal frequency of the (modeled) first aeroelastic mode. As a result of this large uncertainty, it may be quite difficult to meet stability and performance robustness requirements for the feedback systems for these vehicles. Furthermore, in cases for which the system is not square, which may frequently occur, two criteria for robustness must be utilized when an unstructured uncertainty model is used for robustness analysis. But because the criteria are sufficient and not necessary, satisfaction of only one of these conditions guarantees robustness.

In spite of the large uncertainty at the aeroelastic mode frequency, assuming the vehicle to be rigid introduces greater (and unacceptable) uncertainty in the model. This, along with the fact that robustness criteria depend on the size of the uncertainty, indicates that a rigid-body assumption would not appear appropriate for this class of vehicle. Furthermore, robustness properties of multivariable control laws obtained through the use of a nominally rigid-body vehicle model and an uncertainty model that does not consider unmodeled structural dynamics will almost certainly not be valid.

Appendix A: Linear System Model

$$\dot{\boldsymbol{x}} = A\boldsymbol{x} + B\boldsymbol{u}, \qquad \boldsymbol{y} = C\boldsymbol{x} + D\boldsymbol{u}$$

with the state, control, and output vectors defined as

$$\boldsymbol{x} = \begin{bmatrix} h\ (\text{ft}) \\ u\ (\text{ft/s}) \\ \alpha\ (\text{rad}) \\ \theta\ (\text{rad}) \\ q\ (\text{rad/s}) \\ \eta\ (-) \\ \dot{\eta}\ (1/\text{s}) \end{bmatrix}, \qquad \boldsymbol{u} = \begin{bmatrix} \delta_{\text{pitch}}\ (\text{rad}) \\ A_d\ (-) \\ \dot{m}_f\ (\text{slug/s}) \end{bmatrix}, \qquad \boldsymbol{y} = \begin{bmatrix} \alpha_m\ (\text{rad}) \\ q_f\ (\text{rad/s}) \\ q_a\ (\text{rad/s}) \\ P_2\ (\text{atm}) \\ M\ (-) \\ \text{Th}_{\text{eng}}\ (\text{lb/ft}) \\ n_x\ (g) \\ n_z\ (g) \end{bmatrix}$$

$$A = \begin{bmatrix} 0 & 0 & -7.9248e{+}03 & 7.9248e{+}03 & 0 & 0 & 0 \\ 1.5026e{-}04 & -3.2374e{-}03 & -5.2818e{+}01 & -3.2200e{+}01 & 2.3762e{-}02 & 5.7314e{-}01 & 7.5583e{-}03 \\ 1.1744e{-}07 & -3.1848e{-}07 & -3.3921e{-}02 & 0 & 1 & 1.4681e{-}04 & 2.8801e{-}06 \\ 0 & 0 & 0 & 0 & 1 & 0 & 0 \\ -5.7586e{-}06 & -9.6079e{-}06 & 1.5833e{+}00 & 0 & -5.1609e{-}02 & 9.2411e{-}02 & -1.8285e{-}04 \\ 0 & 0 & 0 & 0 & 0 & 0 & 1 \\ -7.4858e{-}01 & 1.0158e{-}01 & 2.4280e{+}03 & 0 & -7.4847e{+}00 & -3.1086e{+}02 & -9.4975e{-}01 \end{bmatrix}$$

$$C = \begin{bmatrix} 0 & 0 & 1 & 0 & 0 & 1.7453e{-}02 & 0 \\ 0 & 0 & 0 & 0 & 1 & 0 & 1.7453e{-}02 \\ 0 & 0 & 0 & 0 & 1 & 0 & -1.7453e{-}02 \\ -4.6971e{-}05 & 2.0641e{-}04 & 6.2428e{+}00 & 0 & -1.0921e{-}02 & 1.0896e{-}01 & 0 \\ -5.3709e{-}06 & 1.0095e{-}03 & 0 & 0 & 0 & 0 & 0 \\ -3.5754e{-}01 & 6.0213e{-}01 & 1.8399e{+}04 & 0 & -3.2185e{+}01 & 3.2112e{+}02 & 0 \\ 4.6665e{-}06 & -1.0054e{-}04 & -1.6403e{+}00 & 0 & 7.3794e{-}04 & 1.7799e{-}02 & 2.3473e{-}04 \\ -2.8902e{-}05 & 7.8381e{-}05 & 8.3483e{+}00 & 0 & -9.8275e{-}03 & -3.6132e{-}02 & -7.0883e{-}04 \end{bmatrix}$$

$$B = \begin{bmatrix} 0 & 0 & 0 \\ -6.4349e{+}01 & -7.4619e{+}01 & 1.7175e{+}02 \\ -1.4482e{-}02 & -1.5955e{-}02 & -3.0690e{-}03 \\ 0 & 0 & 0 \\ -2.4548e{+}00 & 8.1106e{-}01 & 7.0711e{-}01 \\ 0 & 0 & 0 \\ 6.7395e{+}02 & -2.9252e{+}01 & 3.0100e{+}01 \end{bmatrix}, \qquad D = \begin{bmatrix} 0 & 0 & 0 \\ 0 & 0 & 0 \\ 0 & 0 & 0 \\ 0 & -7.2289e{+}00 & 0 \\ 0 & 0 & 0 \\ 0 & -3.1581e{+}04 & 8.1676e{+}04 \\ -1.9984e{+}00 & -2.3174e{+}00 & 5.3337e{+}00 \\ 3.5643e{+}00 & 3.9266e{+}00 & 7.5531e{-}01 \end{bmatrix}$$

Appendix B: Structured Uncertainty Model

$$U_1 = \begin{bmatrix} 0 & 0 & 6.7709e{-}12 & -1.5884e{-}09 & 0 & 0 & 0 \\ 4.8967e{-}02 & -9.8651e{-}01 & 1.5619e{-}01 & -2.2723e{-}03 & -9.4453e{-}02 & 9.9553e{-}01 & -2.3734e{-}03 \\ 1.4397e{-}05 & -2.7359e{-}04 & -1.6279e{-}02 & -9.9987e{-}01 & -2.1179e{-}05 & 1.7756e{-}05 & -1.3655e{-}02 \\ 0 & 0 & 0 & 0 & 0 & 0 & 0 \\ -7.3835e{-}04 & -1.5643e{-}01 & -9.8756e{-}01 & 1.6121e{-}02 & -3.6395e{-}03 & 2.0392e{-}03 & 9.9990e{-}01 \\ 0 & 0 & 0 & 0 & 0 & 0 & 0 \\ -9.9880e{-}01 & -4.8248e{-}02 & 8.3873e{-}03 & -1.3773e{-}04 & 9.9552e{-}01 & 9.4461e{-}02 & 3.4300e{-}03 \end{bmatrix}$$

$$\begin{bmatrix} 0 & 0 & 0 & 0 & 0 & 0 & 0 & 0 & 0 & 0 & 0 & 0 & 0 \\ 0 & 0 & 0 & 0 & 0 & 0 & 1.6933e{-}05 & 9.9852e{-}01 & 5.4466e{-}02 & 0 & 0 & 5.2927e{-}05 & 9.9927e{-}01 \\ 0 & 0 & 0 & 0 & 0 & 0 & 2.5997e{-}09 & 1.5330e{-}04 & -9.2115e{-}03 & 0 & 0 & 1.0459e{-}08 & 1.9748e{-}04 \\ 0 & 0 & 0 & 0 & 0 & 0 & 0 & 0 & 0 & 0 & 0 & 0 & 0 \\ 0 & 0 & 0 & 0 & 0 & 0 & -9.2363e{-}07 & -5.4466e{-}02 & 9.9847e{-}01 & 0 & 0 & 2.0203e{-}06 & 3.8144e{-}02 \\ 0 & 0 & 0 & 0 & 0 & 0 & 0 & 0 & 0 & 0 & 0 & 0 & 0 \\ 0 & 0 & 0 & 0 & -1 & -1 & -1.0000e{+}00 & 1.6958e{-}05 & 0 & 0 & 0 & -1.0000e{+}00 & 5.2965e{-}05 \end{bmatrix}$$

$$\begin{bmatrix} 0 & 0 & 0 \\ 3.8144e{-}02 & 0 & 0 \\ -6.2197e{-}03 & 0 & 0 \\ 0 & 0 & 0 \\ -9.9925e{-}01 & 0 & 0 \\ 0 & 0 & 0 \\ -5.3777e{-}12 & 1 & 0 \end{bmatrix}$$

$$U_2 = \begin{bmatrix} 0 & 0 & 0 & 0 & 0 & 0 & 0 & 0 & 0 & 0 & 0 & 0 & 0 & 0 & 0 \\ 0 & 0 & 0 & 0 & 0 & 0 & 0 & 0 & 0 & 0 & 0 & 0 & 0 & 0 & 0 \\ 0 & 0 & 0 & 0 & 0 & 0 & 0 & 0 & 0 & 0 & 0 & 0 & 0 & 0 & 0 \\ 0 & 0 & 0 & 0 & 0 & 0 & 0 & -5.5289e{-}05 & -1.0000e{+}00 & 4.6506e{-}05 & -1.0000e{+}00 & 0 & 0 & 0 & 0 \\ 0 & 0 & 0 & 0 & 0 & 0 & 0 & 0 & 0 & 0 & 0 & 0 & 0 & 0 & 0 \\ 0 & 0 & 0 & 0 & 0 & 0 & 0 & 1.0000e{+}00 & -5.5289e{-}05 & 1.0000e{+}00 & 4.6506e{-}05 & 0 & 0 & 0 & 0 \end{bmatrix}$$

$$\begin{bmatrix} 0 & 5.4352e{-}05 & 0 & 0 & 0 & 0 & 0 & 0 \\ 0 & 0 & 0 & 0 & 0 & 0 & 0 & 1 \\ 0 & 0 & 0 & 0 & 0 & 0 & 0 & 0 \\ 0 & 3.3931e{-}04 & 0 & 0 & 0 & 0 & 0 & 0 \\ 0 & 0 & 0 & 0 & 0 & 0 & 0 & 0 \\ 0 & 1.0000e{+}00 & 0 & 0 & 0 & 0 & 0 & 0 \end{bmatrix}$$

$$V_1 = \begin{bmatrix} 2.7446e{-}04 & -4.7870e{-}04 & 8.1498e{-}05 & -1.2947e{-}06 & 0 & 0 & 0 & 1.9133e{-}01 & -5.6838e{-}05 & 0 & 0 \\ -1.0045e{-}01 & -9.4094e{-}04 & 1.8222e{-}04 & -3.0509e{-}06 & 0 & 0 & 0 & 4.6541e{-}01 & -4.0129e{-}05 & 0 & 0 \\ -2.4120e{+}03 & 4.0022e{-}03 & -3.2770e{-}07 & -7.8076e{-}10 & 0 & 0 & 0 & 9.1043e{+}03 & 3.2448e{-}09 & 0 & 0 \\ 0 & 0 & 0 & 0 & 0 & 0 & 0 & 0 & 0 & 0 & 0 \\ 7.4459e{+}00 & 3.0293e{-}01 & -9.4385e{-}04 & -4.6303e{-}06 & 0 & 0 & 0 & -1.5926e{+}01 & -5.6763e{-}12 & 0 & 0 \\ -1.2802e{+}01 & -5.7778e{-}01 & -4.9881e{-}04 & -2.3670e{-}06 & 0 & 0 & 0 & 1.5890e{+}02 & 5.6633e{-}11 & 0 & 0 \\ 2.2984e{-}01 & 3.6572e{-}03 & -5.6586e{-}04 & 8.6410e{-}06 & 0 & 0 & 0 & 0 & 0 & 0 & 0 \end{bmatrix}$$

$$\begin{bmatrix} 0 & 0 & 7.4139e{-}01 & -1.2572e{-}05 & 3.3085e{-}13 & 0 \\ 0 & 0 & -6.3512e{-}02 & 1.0770e{-}06 & -2.8343e{-}14 & 0 \\ 0 & 0 & -1.5744e{+}03 & 2.6698e{-}02 & -7.0257e{-}10 & 0 \\ 0 & 0 & 0 & 0 & 0 & 0 \\ 0 & 0 & 1.2620e{+}01 & -2.1400e{-}04 & 5.6317e{-}12 & 0 \\ 6.4800e{+}02 & 0 & -5.5238e{+}01 & -7.6093e{-}01 & -7.3172e{-}07 & 3.2112e{+}02 \\ 7.2000e{-}01 & 7.2000e{-}01 & 3.4438e{-}01 & 4.6174e{-}03 & -1.2058e{-}04 & 0 \end{bmatrix}$$

$$\begin{bmatrix} 0 & 7.1955e{-}03 & -3.8112e{-}07 & 3.8696e{-}14 & 0 & 0 \\ 0 & -3.8066e{-}02 & 2.0162e{-}06 & -2.0471e{-}13 & 0 & 0 \\ 0 & -8.5365e{+}02 & 4.5214e{-}02 & -4.5907e{-}09 & 0 & 0 \\ 0 & 0 & 0 & 0 & 0 & 0 \\ 0 & -5.1351e{+}00 & 2.7198e{-}04 & -2.7615e{-}11 & 0 & 0 \\ 0 & 2.8949e{+}01 & 1.3333e{+}00 & 1.6983e{-}07 & 0 & 0 \\ 1.7453e{-}02 & 1.1511e{-}01 & 2.9474e{-}03 & -7.6753e{-}05 & 0 & -1.7453e{-}02 \end{bmatrix}$$

$$V_2 = \begin{bmatrix} 0 & 0 & 0 & 0 & 6.7702e{+}02 & -4.0364e{-}01 & 9.9944e{-}03 & 0 & 0 & 0 & 0 & 0 \\ 0 & 0 & 0 & 0 & 2.1322e{+}01 & 1.9881e{+}01 & -3.0061e{-}01 & 0 & 0 & 5.7608e{+}03 & -4.7662e{+}00 & 0 \\ 0 & 0 & 0 & 0 & -2.9978e{+}00 & 5.0249e{+}01 & 1.1902e{-}01 & 0 & 0 & 2.4298e{+}04 & 1.1300e{+}00 & 0 \end{bmatrix}$$

$$\begin{bmatrix} 0 & 0 & 0 & 0 & 0 & 0 & 0 & 0 & 0 & 6.7395e{+}02 & 0 \\ 0 & 0 & 0 & 0 & 0 & 0 & 0 & 0 & 0 & -2.9252e{+}01 & 0 \\ 0 & 0 & 0 & 0 & 0 & 0 & 0 & 0 & 0 & 3.0100e{+}01 & 0 \end{bmatrix}$$

Acknowledgments

This research is supported by NASA Langley Research Center under Grant NAG 1-1540. Also, the authors would like to thank the reviewers for their many helpful suggestions, which enhanced the quality and clarity of the paper.

References

[1]Ray, J. K., Carlin, C. M., and Lambregts, A. A., "High-Speed Civil Transport Flight- and Propulsion-Control Technological Issues," NASA CR 186015, March 1992.

[2]"Engine, Airframe Integration Key to Meeting NASP Design Goals," *Aviation Week & Space Technology*, Vol. 133, No. 18, 1990, p. 46.

[3]Chavez, F. R., and Schmidt, D. K., "Analytical Aeropropulsive/Aeroelastic Hypersonic-Vehicle Model with Dynamic Analysis," *Journal of Guidance, Control, and Dynamics*, Vol. 17, No. 6, 1994, pp. 1308–1319.

[4]Lovell, T. A., and Schmidt, D. K., "Effect of Aeropropulsive Interactions and Design Sensitivities on Optimal Hypersonic Ascent Trajectories," AIAA Paper 94-3524, Aug. 1994.

[5]Schmidt, D. K., Mamich, H., and Chavez, F. R., "Dynamics and Control of Hypersonic Vehicles—The Integration Challenge for the 1990's," AIAA Paper 91-5057, Dec. 1991.

[6]Schmidt, D. K., "Integrated Control of Hypersonic Vehicles," AIAA Paper 93-5091, Dec. 1993.

[7]Gregory, I. M., Chowdhry, R. S., McMinn, J. D., and Shaughnessy, J. D., "Hypersonic Vehicle Model and Control Law Development Using H_∞ and μ Synthesis," NASA TM 4562, Oct. 1994.

[8]Thompson, P. M., Myers, T. T., and Suchomel, C., "Conventional Longitudinal Axis Autopilot Design for a Hypersonic Vehicle," AIAA Paper 95-0556, Jan. 1995.

[9]Myers, T. T., Klyde, D. H., McRuer, D. T., and Suchomel, C. F., "Influence of Path-Attitude Lag in Hypersonic Flying Qualities," AIAA Paper 95-0555, Jan. 1995.

[10]Schierman, J., and Schmidt, D. K., "Analysis of Airframe and Engine Control Interactions and Integrated Flight/Propulsion Control," *Journal of Guidance, Control, and Dynamics*, Vol. 15, No. 6, 1992, pp. 1388–1396.

[11]Schmidt, D. K., "On the Integrated Control of Flexible Supersonic Transport Aircraft," AIAA Paper 95-3200, Aug. 1995.

[12]McGruer, D., "Design and Modeling Issues for Integrated Airframe/Propulsion Control of Hypersonic Flight Vehicles," *Proceedings of the American Control Conference*, Vol. 1, 1991, pp. 729–734.

[13]Tarpley, C., and Lewis, M. J., "Stability Derivatives for a Hypersonic Caret-Wing Waverider," *Journal of Aircraft*, Vol. 32, No. 4, 1995, pp. 795–800.

[14]Shaughnessy, J. D., Pinckney, S. Z., McMinn, J. D., Cruz, C. I., and Kelley, M., "Hypersonic Vehicle Simulation Model: Winged-Cone Configuration," NASA TM-102610, Nov. 1990.

[15]Raney, D. L., McMinn, J. D., and Pototzky, A. S., "Impact of Aeroelastic-Propulsive Interactions of Flight Dynamics of a Hypersonic Vehicle," *Journal of Aircraft*, Vol. 32, No. 2, 1995, pp. 355–360.

[16]Dress, D. A., Boyden, R. P., and Cruz, C. I., "Measured and Theoretical Supersonic Dynamic Stability Characteristics of a National Aero-Space Plane Configuration," *Journal of Aircraft*, Vol. 31, No. 3, 1994, pp. 597–602.

[17]Maciejowski, J. M., *Multivariable Feedback Design*, Addison–Wesley, Reading, MA, 1989.

[18]Morari, M., and Zafiriou, E., *Robust Process Control*, Prentice–Hall, Englewood Cliffs, NJ, 1989.

[19]Zhou, K., Doyle, J. C., and Glover, K., *Robust and Optimal Control*, Prentice–Hall, Englewood Cliffs, NJ, 1996.

[20]Sofonov, M. G., "Stability Margins of Diagonally Perturbed Multivariable Feedback Systems," *Proceedings of the IEEE Conference on Decision and Control*, Pt. D, 1982, pp. 251–256.

[21]Wise, K. A., "Missile Autopilot Robustness Using the Real Multiloop Stability Margin," *Journal of Guidance, Control, and Dynamics*, Vol. 16, No. 2, 1993, pp. 354–362.